

Ferrocenophanes with Interannular Boron–Phosphorus Bridges: Synthesis, Structure, and Reactivity toward Nitrogen Bases

Eberhardt Herdtweck, Frieder Jäkle, and Matthias Wagner*

Anorganisch-Chemisches Institut der Technischen Universität München,
Lichtenbergstrasse 4, D-85747 Garching, Germany

Received June 9, 1997[⊗]

Starting from readily available diborylferrocenes 1,1'-fc[B(Br)R]₂ (fc = (C₅H₄)Fe(C₅H₄); R: Br (**1a**), Me (**1b**), OEt (**1d**)), ferrocenophanes 1,1'-fc[B(μ -PPh₂)R]₂ (R = Br (**2a**), Me (**2b**), PPh₂ (**2d**)) and 1,1'-fc[B(μ -PPh₂)OEt][B(μ -PPh₂)PPh₂] (**2c**) are obtained upon reaction with LiPPh₂. In contrast, 1,1'-fc[B(Br)pyr]₂ (pyr = pyrrolidinyll, **1e**) and 2 equiv of LiPPh₂ give an open-chain ferrocene 1,1'-fc[B(PPh₂)pyr]₂ (**2e**). The dynamic behavior of the B₂P₂-bridged species has been investigated using variable-temperature NMR spectroscopy and the Forsén–Hoffman spin saturation transfer method. The reaction of **2a** with Lipz (pz = pyrazolide) gives the *ansa*-ferrocene 1,1'-fc[B(μ -PPh₂)PPh₂][B(μ -pz)Br] (**3a**), featuring an interannular (BNNBP) heterocyclic bridge. When Lipz* (pz* = 4-bromo-3,5-dimethylpyrazolide) was used rather than Lipz, two products could be isolated: **3b**, which is analogous to **3a**, and 1,1'-fc[B(μ -PPh₂)Br][B(μ -pz)Br] (**3c**), which bears Br substituents at both bridgehead boron centers. **2d** and **3c** have been characterized by X-ray crystallography. Treatment of **2a** with excess γ -picoline (pic) results in an *ansa*-bridge opening and bromide substitution with the formation of the ionic species {1,1'-fc[B(PPh₂)pic₂]₂}Br₂ (**5a**). The presence of three-coordinate phosphorus centers in **5a** was confirmed by showing their ability to bind Cr(CO)₅ fragments, which afforded the trimetallic complex **5b**.

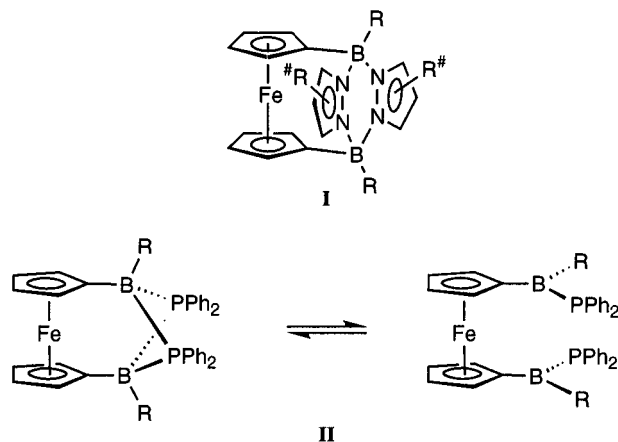
Introduction

We have recently shown that the combination of Lewis-acidic boron centers with Lewis-basic amino or phosphino substituents in the ligand sphere of the same ferrocene molecule can lead to interannular donor–acceptor bonding and, thus, to ferrocenophanes **I** and **II** (Scheme 1).^{1–4}

This approach to *ansa*-bridged sandwich complexes has an advantage due to the facile formation of dative boron–nitrogen(phosphorus) links. Moreover, donor–acceptor bonds may be broken and re-formed reversibly without affecting the rest of the molecule. Our aim is to make ferrocenophanes with “switchable” *ansa*-bridges, which may be opened either by being thermally induced or with the help of electrophilic or nucleophilic additives (Scheme 1). While most *ansa*-ferrocenes **I** with a pyrazabole⁵ bridge possess particularly rigid molecular geometries, a continuous breaking and re-forming of the interannular B₂P₂ ring of **II** (R = Me) was detected by NMR spectroscopy even at ambient temperature.⁴

The purpose of this paper is to give more detailed information about the influence of substituents at boron

Scheme 1. Ferrocenophanes with a Pyrazabole (I) and B₂P₂ Bridge (II)^a



^a The monomer–dimer equilibrium of the phosphinoboryl substituents in **II** (R = Me) causes continuous breaking and re-forming of the *ansa*-bridge.

on the strength of the interannular B–P bonds and to investigate the reactivity of derivatives **II** toward selected Lewis bases. Special emphasis will be put on the relative stabilities of the bridging units in **I** and **II**.

Results and Discussion

Syntheses. *ansa*-Ferrocenes **2a** and **2b** are prepared by reaction of **1a** and **1b** with 2 equiv of LiPPh₂ in 50% and 80% yield, respectively (Scheme 2).⁴ *ansa*-Bridge formation in **2a** and **2b** is the result of an intramolecular dimerization of two phosphinoborane moieties *via* dative B–P bonds. Such links are known to be weakened by the presence of π donor substituents at boron.⁶ We

* Author to whom correspondence should be addressed. Telefax: +49-89-28913473. E-mail: wagner@arthur.anorg.chemie.tu-muenchen.de.

[⊗] Abstract published in *Advance ACS Abstracts*, September 15, 1997.

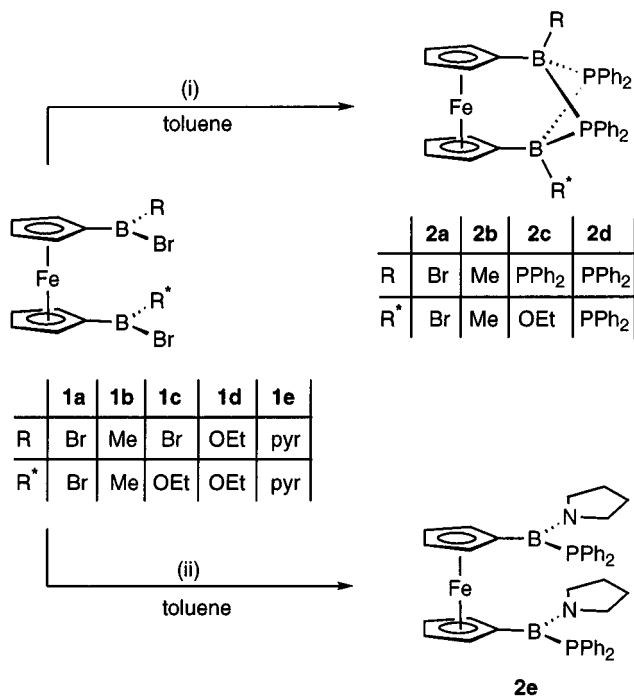
(1) Jäkle, F.; Priermeier, T.; Wagner, M. *J. Chem. Soc., Chem. Commun.* **1995**, 1765–1766.

(2) Herdtweck, E.; Jäkle, F.; Opromolla, G.; Spiegler, M.; Wagner, M.; Zanello, P. *Organometallics* **1996**, *15*, 5524–5535.

(3) Jäkle, F.; Priermeier, T.; Wagner, M. *Organometallics* **1996**, *15*, 2033–2040.

(4) Jäkle, F.; Mattner, M.; Priermeier, T.; Wagner, M. *J. Organomet. Chem.* **1995**, *502*, 123–130.

(5) Trofimenko, S. *J. Am. Chem. Soc.* **1967**, *89*, 4948–4952.

Scheme 2^a

^a Key: (i) **2a**: **1a** + 2LiPPh₂; **2b**: **1b** + 2LiPPh₂; **2c**: **1c** + 3LiPPh₂; **2d**: **1a** + 4LiPPh₂. (ii) **1e** + 2LiPPh₂. All reactions: toluene, -78 °C to ambient temperature.

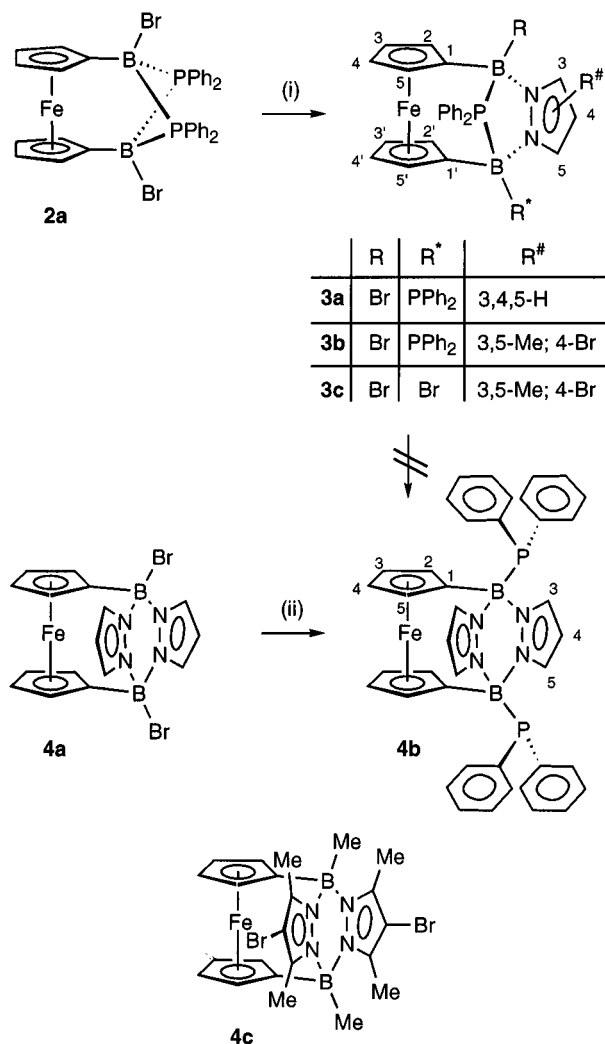
were, thus, interested in derivatives of **2** bearing ethoxy (R = R^{*} = OEt) and pyrrolidine substituents (R = R^{*} = pyr) at boron (Scheme 2). These should gradually increase the electron density at the boron centers and in turn shift the equilibrium between the *ansa*-bridged and the open-chain ferrocene to the right side (**II**; Scheme 1).

An attempted synthesis of the ethoxy derivative from **1d** and 2 equiv of LiPPh₂ yielded a mixture of different products. Only the unsymmetrically substituted **2c** could be isolated in pure form (Scheme 2). Similar results were obtained when HPPH₂/NEt₃ was employed instead of LiPPh₂.

The yield of **2c** could be increased considerably by reacting **1c**, which was prepared *in situ* from **1a** and one equiv of diethyl ether, with 3 equiv of LiPPh₂. Again, substitution of the ethoxy group for PPh₂ took place to some extent, leading to **2d** as a byproduct. The chemical composition of this material was confirmed by preparing an authentic sample of **2d** from **1a** and 4 equiv of LiPPh₂. Compared to **2a** and **2b**, which are extremely moisture sensitive, **2c** is much more stable and **2d**, which bears four sterically demanding PPh₂ substituents, may even be handled in air for short periods of time. X-ray quality crystals of **2d** were grown from toluene/hexane (1:1) at -25 °C. Finally, the reaction of **1e** with 2 equiv of LiPPh₂ affords open-chain **2e** in good yield.

Treatment of **2a** with 1 equiv of lithium pyrazolide (Lipz) in toluene/THF leads to the displacement of one μ -PPh₂ unit by a pyrazole ring to give the ferrocenophane **3a**, which is the missing link between structures **I** and **II** (Scheme 1, 3).

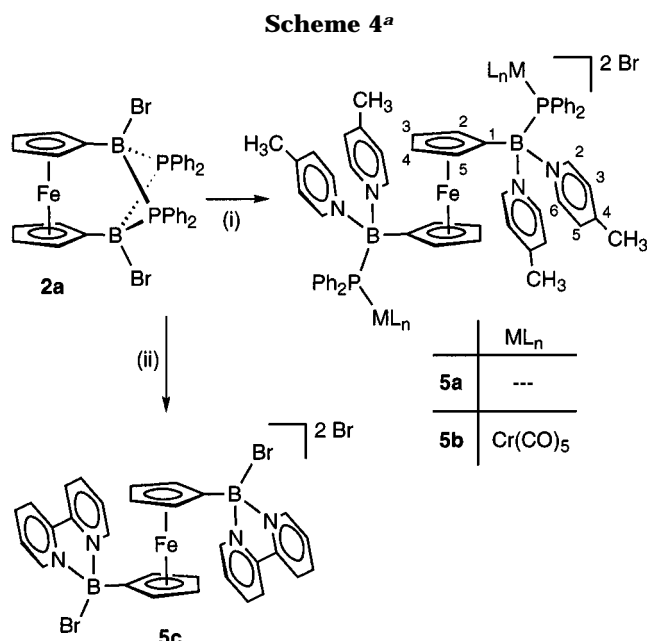
In our experience, ferrocenophanes **I** with bridging pz^{*} units (pz^{*} = 4-bromo-3,5-dimethylpyrazolide) usu-

Scheme 3^a

^a Key: (i) **3a**: **2a** + Lipz, toluene/THF, -78 °C to ambient temperature; **3b,c**: **2a** + Lipz^{*}, toluene/diethyl ether, ambient temperature. (ii) **4a** + 2LiPPh₂, toluene, 12 h reflux.

ally give single crystals of particular good quality.¹ To gain detailed structural information about the unique (BNNBP) heterocycle of **3**, the reaction was, thus, repeated using Lipz^{*} instead of the parent Lipz. Two products **3b** and **3c** were obtained in a ratio of 2:1, both of them featuring the aimed-for unsymmetrical interannular bridge. **3b**, which bears two different exocyclic boron substituents, results from the expected elimination of LiBr, while the minor product **3c** is formed by substitution of PPh₂ (Scheme 3). Ferrocenophane **3c** gave crystals suitable for an X-ray crystal structure investigation. Even with a large excess of the nucleophile (2.5 equiv), the reaction of **3a** with Lipz does not proceed further to the pyrazabole derivative **4b**. However, **4b** is accessible in high yield *via* a different pathway starting from **4a** and 2 equiv of LiPPh₂ (Scheme 3).

While **2d** does not react with γ -picoline, treatment of the methyl derivative **2b** with 2 equiv, 4 equiv, or a large excess of this base led to slow ferrocenophane degradation (ambient temperature; toluene). In contrast, when **2a** is dissolved in neat γ -picoline, the open-chain species **5a** forms almost quantitatively within 30 min. Bromide substitution takes place in addition to the cleavage of



^a Key: (i) **5a**: **2a** + excess γ -picoline, ambient temperature; **5b**: **5a** + excess Cr(CO)₅/THF, toluene/CH₂Cl₂/THF, ambient temperature. (ii) **2a** + 2bipy, CH₂Cl₂, ambient temperature.

two B–P bonds, generating tetracoordinate boronium cations (Scheme 4).

The presence of three-coordinate phosphorus centers in **5a** was proven by showing their ability to bind Cr(CO)₅ fragments, which afforded the trimetallic complex **5b**. The stability of the proposed ferrocenyl-boronium cations can be expected to increase when each of the two picoline donors are substituted for one chelating 2,2'-bipyridine ligand (bipy). We have, therefore, investigated the reaction of **2a** with 2 equiv of bipy both in toluene and in CH₂Cl₂ solution. From toluene, a deep purple microcrystalline solid gradually precipitated, which was poorly soluble in all common aprotic solvents. Its ¹H NMR data revealed a very complex mixture of degradation products. In CH₂Cl₂, the reaction is still rather unselective. Nevertheless, isolation and characterization of one product (**5c**) was achieved (Scheme 4). The chemical composition of the dication **5c** was confirmed by a comparison of its NMR resonances with those of an authentic sample prepared from **1a** and 2 equiv of bipy.⁷ The fact that a PPh₂ substituent may be replaced preferentially to Br by the bipy ligand is reminiscent of the formation of **3c** from **2a** and Lipz*.

NMR Spectroscopy. The ¹¹B NMR spectra of **2c** and **2d** show resonances in a range characteristic for tetracoordinate boron nuclei⁸ (**2c**, –8.4, 11.2 ppm; **2d**, –2.4 ppm). The fact that two signals (integral ratio 1:1) are observed in the case of **2c** is in agreement with the low symmetry of its proposed molecular structure. We tentatively assign the resonance at –8.4 ppm to the boron atom bearing an *exo*-PPh₂ substituent, since this value is closer to the one found for **2d** ($\delta(^{11}\text{B}) = -2.4$). The pyrrolidine derivative **2e** features only one signal at $\delta(^{11}\text{B}) = 42.9$, indicating three-coordinate rather than

four-coordinate boron centers.⁸ The ¹¹B NMR signals of **2c–e** are broad ($h_{1/2}$ between 250 and 500 Hz), thus ¹J(B,P) coupling is not resolved. In the ³¹P NMR spectra of **2c** and **2d**, the resonances for the μ -PPh₂ units appear at $\delta(^{31}\text{P}) = -14.1$ and -4.3 , respectively, which is the region usually observed for dimeric phosphinoboranes.^{9–15} In both cases, the signals for the exocyclic PPh₂ substituents are found at higher field compared to the bridging phosphorus atoms (**2c** $\delta(^{31}\text{P}) = -55.3$, ²J(P,P) = 35 Hz; **2d** $\delta(^{31}\text{P}) = -57.9$, ²J(P,P) = 31 Hz) with integral ratios of *exo*-P: μ -P = 1:2 and 2:2, respectively. The ³¹P NMR spectrum of **2e** shows one sharp resonance at $\delta(^{31}\text{P}) = -39.8$ ($h_{1/2} = 50$ Hz), which is very close to the value reported for the parent HPPH₂ ($\delta(^{31}\text{P}) = -41.1$).¹⁶ This again suggests an open-chain configuration of **2e** in solution.

Mutual assignments of the ¹H and ¹³C resonance signals are based on 2D heteronuclear shift correlations. Together with ¹H/¹H COSY and NOE difference spectra, an almost complete assignment of the resonances was achieved. The ¹H NMR signals of **2c–e** appear in the usually observed ranges. The ferrocene backbone of **2c** gives rise to three proton resonances (integral ratio 2:4:2), whereas only two such signals are present in **2d** and **2e**. This finding can easily be explained by the reduced symmetry of **2c**, which bears two different substituents at its bridgehead boron atoms. In the aromatic regions of their ¹H NMR spectra, three sets of signals are observed for **2c** (integral ratio 2:2:2) and **2d** (integral ratio 4:2:2). It may be concluded that in both cases the exocyclic phenyl rings are magnetically equivalent. In contrast, those of the bridging PPh₂ units have different chemical environments, because the phosphorus centers are locked between two boron atoms. The NMR pattern described is, thus, an important characteristic for the rigid B₂P₂ *ansa*-structures. Consequently, the ¹H NMR spectrum of **2e** features only one set of phenyl resonances, which points toward a largely unrestricted rotation about the B–P axis and is in agreement with the proposed open-chain conformation of this compound. Four different proton signals for the pyrrolidine substituents of **2e** show the B–N rotation to be slow on the NMR time scale as a result of pronounced N–B π bonding to the three-coordinate boron nuclei. In the ¹³C NMR spectra of **2c–e**, signal patterns very similar to those discussed for the proton spectra are observed and the same arguments hold for their interpretation.

The ¹¹B NMR data of all derivatives **3** are symptomatic of boron centers coordinated by four substituents (**3a**, –2.1 ppm; **3b**, –2.3 ppm; **3c**, –3.0 ppm).⁸ Spin–spin coupling between the ¹¹B and ³¹P nuclei is not resolved. Two signals of equal intensity are apparent in the ³¹P NMR spectra of **3a** (–46.6, 0.9 ppm) and **3b** (–43.7, –6.3 ppm), whereas only one resonance is found for **3c** (–10.0

(9) Nöth, H. *Z. Anorg. Allg. Chem.* **1987**, *555*, 79–84.

(10) Köster, R.; Seidel, G.; Müller, G.; Boese, R.; Wrackmeyer, B. *Chem. Ber.* **1988**, *121*, 1381–1392.

(11) Bartlett, R. A.; Dias, H. V. R.; Feng, X.; Power, P. P. *J. Am. Chem. Soc.* **1989**, *111*, 1306–1311.

(12) Karsch, H. H.; Hanika, G.; Huber, B.; Riede, J.; Müller, G. *J. Organomet. Chem.* **1989**, *361*, C25–C29.

(13) Frankhauser, P.; Driess, M.; Pritzkow, H.; Siebert, W. *Chem. Ber.* **1992**, *125*, 1341–1350.

(14) Nöth, H.; Staude, S.; Thomann, M.; Paine, R. T. *Chem. Ber.* **1993**, *126*, 611–618.

(15) Groshens, T. J.; Higa, K. T.; Nissan, R.; Butcher, R. J.; Freyer, A. J. *Organometallics* **1993**, *12*, 2904–2910.

(16) Berger, S.; Braun, S.; Kalinowski, H.-O. *³¹P-NMR-Spektroskopie*; G. Thieme Verlag: Stuttgart, New York, 1993.

(7) Fabrizi de Biani, F.; Gmeinwieser, T.; Herdtweck, E.; Jäkle, F.; Laschi, F.; Wagner, M.; Zanella, P. *Organometallics*, in press.

(8) Nöth, H.; Wrackmeyer, B. *Nuclear Magnetic Resonance Spectroscopy of Boron Compounds*. In *NMR Basic Principles and Progress*; Diehl, P., Fluck, E., Kosfeld, R., Eds.; Springer: Berlin, 1978; Vol. 14.

ppm). ^{31}P – ^{31}P coupling leads to a doublet structure of the more shielded ^{31}P NMR signals of **3a** and **3b**, the coupling constants being 50 and 40 Hz, respectively. $^2J(\text{P},\text{P})$ coupling is not resolved in the case of the much broader signals at $\delta(^{31}\text{P}) = 0.9$ ($h_{1/2} = 300$ Hz; **3a**) and -6.3 ($h_{1/2} = 300$ Hz; **3b**). On the basis of their different line shapes and by comparison with the ^{31}P NMR shifts of **2d** ($\delta(\mu\text{-P}) = -4.3$; $\delta(\text{exo-P}) = -57.9$), **3c** ($\delta(\mu\text{-P}) = -10.0$), and **4b** ($\delta(\text{exo-P}) = -39.3$), the signals at higher field most likely have to be assigned to the exocyclic PPh_2 groups of **3a** and **3b** whereas the signals at 0.9 ppm and -6.3 ppm correspond to the bridging phosphorus atoms. The ^1H and ^{13}C NMR spectra of **3a** and **3b** each reveal eight signals in the ferrocene region and, thus, indicate that these molecules possess no elements of symmetry. In contrast, **3c** shows only four proton and four carbon resonances due to a symmetry plane that runs through the iron atom and is coplanar to the cyclopentadienyl rings of the ferrocene backbone. The ^1H chemical shifts of the ferrocene moieties in **3a**–**c** noticeably reflect the different nature of the two bridging units: Protons adjacent to $\mu\text{-PPh}_2$ are only slightly more shielded than those of the parent ferrocene (e.g. **3c** $\delta(^1\text{H}) = 3.82$), which is consistent with the NMR data of **2a**–**d**. On the other hand, a considerable upfield shift is observed for protons adjacent to the pyrazolyl fragment (e.g., **3c** $\delta(^1\text{H}) = 3.36$). This anisotropy effect of the amine heterocycle has already been shown to be operative in ferrocenophanes with a pyrazabole bridge (e.g. **4a,b**).^{1–3} In all three derivatives **3a**–**c** the phenyl rings of $\mu\text{-PPh}_2$ give rise to two sets of resonances both in the ^1H and in the ^{13}C NMR spectra, whereas those of exo-PPh_2 are magnetically equivalent in **3a** as well as in **3b**.

The ^{31}P NMR signal of **4b** at -39.3 ppm appears in the same shift range as those of the exocyclic PPh_2 substituents in **3a** and **3b** (-46.6 and -43.7 ppm, respectively). The NMR spectroscopic data of **4b** show no peculiarities compared to other pyrazabole-bridged ferrocenophanes^{1–3} and, thus, deserve no further discussion.

In the ^{11}B NMR spectrum of **5a**, the resonance at 7.3 ppm testifies to the presence of tetracoordinate boron nuclei.⁸ Compared to the starting material **2a** ($\delta(^{11}\text{B}) = -5.7$),⁴ the boron signal of the picoline adduct **5a** is shifted to lower field by 13.0 ppm. A similar effect is observed in the ^{31}P NMR spectra of both compounds (**2a**, -36.4 ppm; **5a**, -27.4 ppm). Moreover, the ^{31}P NMR signal sharpens up upon going from **2a** ($h_{1/2} = 180$ Hz) to **5a** ($h_{1/2} = 50$ Hz). In contrast to **2a**, the phenyl rings of **5a** are all magnetically equivalent in the ^1H and ^{13}C NMR spectra. From an inspection of the integral ratios in the proton NMR of **5a**, it may be deduced that two PPh_2 moieties and four γ -picoline ligands are present in the molecule. This is in accord with the proposed dicationic nature of **5a** (Scheme 4). Due to spin–spin coupling with one ^{31}P nucleus, the signals of $\text{Cp-C}_{2,5}$ ($^3J(\text{P},\text{C}) = 2.3$ Hz) and $\text{pic-C}_{2,6}$ ($^3J(\text{P},\text{C}) = 7.7$ Hz) appear as doublets in the ^{13}C NMR spectrum. This finding gives conclusive evidence for the open-chain structure of **5a**, since a triplet splitting is observed for the resonances of $\text{Cp-C}_{2,5}$ in *ansa-2a* ($^3J(\text{P},\text{C}) = 8.0$ Hz) and *ansa-2b* ($^3J(\text{P},\text{C}) = 9.0$ Hz).⁴ Moreover, the chemical shift values of **5a** closely resemble those of $\text{Fc}[\text{B}(\text{Me})-$

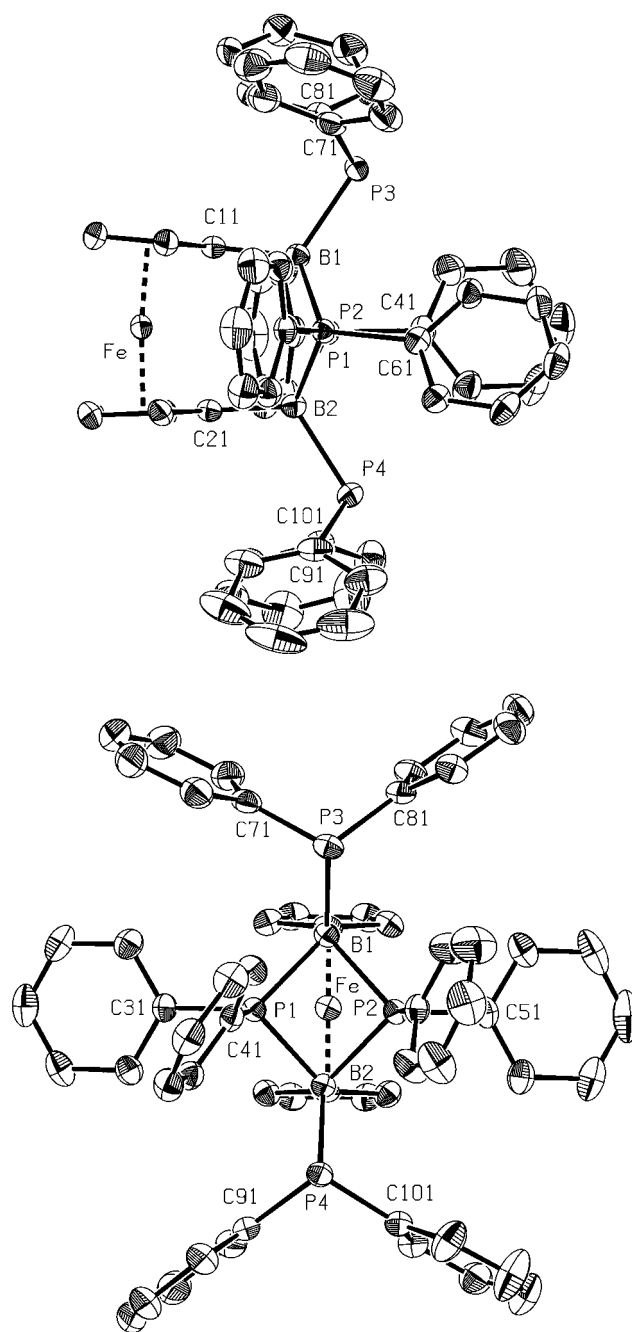


Figure 1. PLATON plot of **2d** (hydrogen atoms and toluene molecules omitted for clarity; thermal ellipsoids at the 50% probability level).

$\text{pic}_2\text{]Br}$ ($\text{Fc} = (\text{C}_5\text{H}_5)\text{Fe}(\text{C}_5\text{H}_4)$), which has recently been described by our group.⁷

The main difference between the NMR spectra of **5a** and the corresponding trimetallic complex **5b** lies in a 46.7 ppm downfield shift of the ^{31}P NMR signal upon $\text{Cr}(\text{CO})_5$ coordination (**5a** $\delta(^{31}\text{P}) = -27.4$; **5b** $\delta(^{31}\text{P}) = 19.3$). Moreover, most ^{31}P – ^{13}C coupling constants are significantly smaller in **5b** than in the free ligand **5a**. The NMR signal of the equatorial carbonyl groups in **5b** is found at $\delta(^{13}\text{C}_{\text{eq}}) = 217.0$ ($^2J(\text{P},\text{C}) = 7.8$ Hz), and the axial CO ligands resonate at $\delta(^{13}\text{C}_{\text{ax}}) = 225.5$.

Molecular Structures of 2d and 3c. **2d** crystallizes from toluene/hexane with 1 equiv of toluene in the monoclinic space group $C2/c$ (Figure 1). Yellow crystals of **3c** (tetragonal; space group $P4_2/m$) were obtained by layering its toluene solution with hexane. The com-

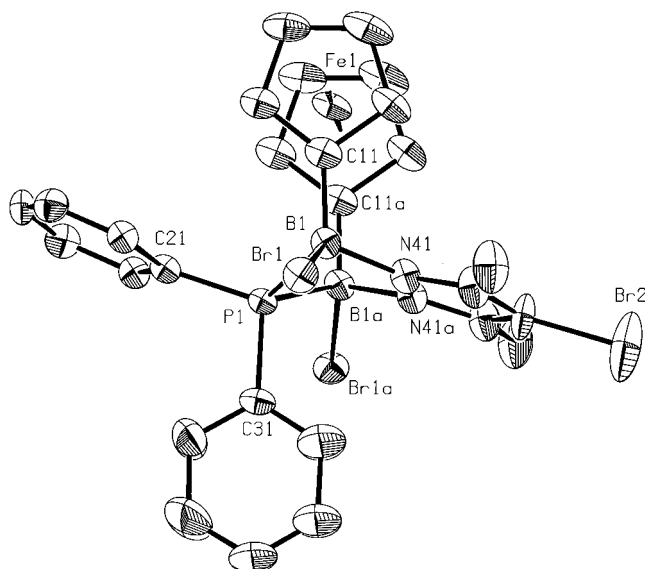


Figure 2. PLATON plot of **3c** (hydrogen atoms and toluene molecules omitted for clarity; thermal ellipsoids at the 50% probability level).

Table 1. Summary of Crystallographic Data for 2d·(toluene) and 3c·0.5(toluene)·0.25(hexane)

compd	2d	3c
formula	C ₅₈ H ₄₈ B ₂ FeP ₄ ·C ₇ H ₈	C ₂₇ H ₂₄ B ₂ Br ₃ FeN ₂ P·0.5C ₇ H ₈ ·(0.25C ₆ H ₁₄)
fw	1038.45	770.72
cryst dimens, mm	0.45 × 0.33 × 0.25	0.43 × 0.25 × 0.13
cryst syst	monoclinic	tetragonal
space group	C2/c (No. 15)	P4 ₂ /m (No. 84)
temp, K	253(2)	193(2)
a, Å	36.522(3)	15.8389(9)
b, Å	13.566(1)	15.8389(9)
c, Å	22.181(2)	12.6240(6)
α, deg	90	90
β, deg	96.133(7)	90
γ, deg	90	90
V, Å ³	10926.8(16)	3167.0(3)
D _{calcd} , g cm ⁻³	1.262	1.617
Z	8	4
F(000)	4336	1524
radiation	Mo Kα, 0.710 73 Å	Mo Kα, 0.710 73 Å
no. of total reflns	61576	14259
no. of unique reflns	9100	2984
no. of obsd reflns	7558 (<i>I</i> > 2σ(<i>I</i>))	1857 (<i>I</i> > 2σ(<i>I</i>))
no. of params	685	200
μ, cm ⁻¹	4.3	43.3
final R1 ^a	0.0566 (all data)	0.0811 (all data)
final wR2 ^b	0.1191 (all data)	0.1483 (all data)
GOF ^c	1.096 (all data)	0.963 (all data)

^a R1 = $\sum(|F_o| - |F_c|)/\sum|F_o|$. ^b wR2 = $[\sum w(F_o^2 - F_c^2)^2/\sum w(F_o^2)^2]^{1/2}$. ^c GOF = $[\sum w(F_o^2 - F_c^2)^2/(\text{NO} - \text{NV})]^{1/2}$.

pound crystallizes together with 1 equiv of toluene and a nonstoichiometric amount of hexane (ca. 0.25 equiv; Figure 2).

A summary of crystallographic data and selected geometrical parameters of **2d** and **3c** is given in Tables 1 and 2. The complete set of structural data is available on request.¹⁷

As already deduced from the NMR data, **2d** bears two *ansa*-bridging and two exocyclic PPh₂ substituents. The

interannular B₂P₂ ring is not planar but adopts a butterfly conformation. The angle between the two halves of the ring which meet in the P···P line is 43.4° (**2b**, 41.6°⁴); for the two halves meeting in the B···B line, an angle of 46.2° is found (**2b**, 45.0°⁴). Most importantly, the two cyclopentadienyl ligands of **2d** deviate only slightly from the coplanar arrangement found in the parent ferrocene (C(11)–C(15)//C(21)–C(25) = 7.8°). It may, thus, be concluded that the *ansa*-bridge of **2d** is able to adjust almost perfectly to the steric requirements of the sandwich complex (for a more detailed discussion of ring conformations in dimeric phosphino-boranes see ref 4 and the literature cited therein). The electron lone pairs of both pendant PPh₂ moieties are directed away from the ferrocene backbone in order to minimize steric interactions between the phenyl rings of *exo*-PPh₂ on one hand and *μ*-PPh₂ on the other. The bond lengths between the boron centers and the three-coordinate *exo*-phosphorus atoms are shorter (B(1)–P(3) = 1.999(3) Å; B(2)–P(4) = 2.001(3) Å) than those found within the bridging B₂P₂ ring, which involve tetracoordinate phosphorus atoms (B(1)–P(1) = 2.034(3) Å; B(1)–P(2) = 2.033(3) Å; B(2)–P(1) = 2.028(3) Å; B(2)–P(2) = 2.047(3) Å). Similar mean values of B–P(*μ*) = 2.036(3) Å and B–P(*exo*) = 2.000(3) Å and differences Δ between B–P(*μ*) and B–P(*exo*) (Δ = 0.036(3) Å) are found in **2d** and in the related unbridged phosphinoborane dimer [B(P*Et*)₂]₂ (B–P(*μ*) = 2.018(6) Å; B–P(*exo*) = 1.973(7) Å; Δ = 0.045(7) Å).^{9,18,19} The sum of angles around P(3) and P(4) in **2d** is 313.8(1)° and 312.6(1)°, respectively.

Compound **3c** features one PPh₂ and one pyrazolyl unit in the *ansa*-bridge. The resulting five-membered heterocycle adopts an *envelope* conformation with the phosphorus atom deviating from the plane spanned by the boron and nitrogen atoms. Again, the Cp rings of the ferrocene backbone are essentially coplanar. The bond lengths and angles within the B–(*μ*-pz)–B fragment of **3c** are very similar to those found in the related pyrazole-bridged derivative **4c** (Table 2).¹ In contrast, the B–P bond lengths are shortened by 0.064 Å (0.060 Å) upon going from **2b** (**2d**) (B–P(*μ*) = 2.040(4) Å (2.036(3) Å)) to **3c** (B(1)–P(1) = 1.976(7) Å). The phenyl ring, C(31)–C(36), of **3c** is located in the symmetry plane of the molecule, which results in an energetically favorable *edge-on* conformation, both with respect to the second phenyl ring (C(21)–C(26)) and the pyrazolyl bridge. This arrangement is not possible in **2b,d** due to the presence of the second sterically demanding PPh₂ moiety.

Conclusion

Three different grades of B–P donor–acceptor bond stability have to be distinguished in compounds **2**. In the case of derivatives **2a** and **2d**, the ¹¹B and ³¹P NMR resonances show essentially unaltered chemical shift values in the temperature range between –60 and +100 °C (toluene-*d*₈). Moreover, two (**2a**) and three (**2d**) magnetically different phenyl rings are always distinguishable in the variable-temperature ¹H and ¹³C NMR spectra. Employing the spin saturation transfer

(17) Further details of the crystal structure investigations are available on request from the Fachinformationszentrum Karlsruhe, Gesellschaft für wissenschaftlich-technische Information mbH, D-76344 Eggenstein-Leopoldshafen, Germany, on quoting the depository numbers CSD 407667 (**2d**), CSD 407668 (**3c**), the names of the authors, and the literature citation.

(18) Fritz, G.; Pfannerer, F. *Z. Anorg. Allg. Chem.* **1970**, *373*, 30–35.

(19) Fritz, G.; Sattler, E. *Z. Anorg. Allg. Chem.* **1975**, *413*, 193–228.

Table 2. Selected Bond Lengths (Å), Angles (deg), and Angles between Planes (deg) of 2d, 3c, and the Reference Compound 4c^a

2d		3c		4c	
B(1)–P(1)	2.034(3)	B(1)–P(1)	1.976(7)		
B(1)–P(2)	2.033(3)				
B(2)–P(1)	2.028(3)				
B(2)–P(2)	2.047(3)				
B(1)–P(3)	1.999(3)	B(1)–Br(1)	2.040(7)	B–C(Me)	1.596
B(2)–P(4)	2.001(3)				
B(1)–C(11)	1.603(4)	B(1)–C(11)	1.589(9)	B–C(Cp)	1.593
B(2)–C(21)	1.597(4)				
		B(1)–N(41)	1.574(8)	B–N(pz)	1.599
		N(41)–N(41a)	1.379(7)	N–N	1.379
P(1)–B(1)–P(2)	81.9(1)				
P(1)–B(2)–P(2)	81.8(1)				
B(1)–P(1)–B(2)	89.4(1)	B(1)–P(1)–B(1)a	91.0(3)		
B(1)–P(2)–B(2)	88.9(1)				
		P(1)–B(1)–N(41)	95.9(4)	N–B–N	105.0
		B(1)–N(41)–N(41a)	117.3(5)	B–N–N	121.2
P(1)B(1)P(2)//P(1)B(2)P(2)	43.4				
B(1)P(1)B(2)//B(1)P(2)B(2)	46.2	B(1)P(1)B(1)a//B(1)N(41)N(41a)B(1)a	46.4	pz//pz'	24.0
C(11)–C(15)//C(21)–C(25)	7.8	C(11)–C(15)//C(11a)–C(15a)	4.9	Cp//Cp'	4.5

^a Mean values are given for **4c**.

method,^{20–22} which provides a means for studying moderately rapid exchange phenomena, it has also been possible to exclude the dynamic behavior of the B–P(μ) bonds in **2a** and **2d** on a slower time scale. This leads to the conclusion that the *ansa*-bridge of these derivatives remains intact under our experimental conditions. In contrast, a very fast breaking and re-forming of B–P bonds is already apparent at ambient temperature in *ansa*-**2b**, even though no detectable stationary concentration of open-chain **2b** builds up.⁴ The different dynamic behavior of **2a** and **2b** may be attributed to the different electronegativities of the Br and CH₃ substituents. The presence of electron-withdrawing bromine atoms in **2a** increases the Lewis acidity of the bridgehead boron centers and in turn strengthens the interannular B–P bonds.²³ One may also anticipate kinetic hindrance of the B₂P₂ bridge fluxionality to occur when sterically demanding groups are attached to the boron centers, and this factor certainly contributes to the rigidity of *ansa*-**2d**.

The pyrrolidine derivative **2e** maintains an open-chain structure even upon cooling to –80 °C (NMR spectroscopy; toluene-*d*₈). A N–B π interaction obviously prevents effective attachment of the phosphine bases to the boron centers and, thus, *ansa*-bridge formation, although this would be a favorable *intra*-molecular process.

Ferrocenophanes **2** with R = R* = OEt (Scheme 2) have not been synthetically accessible in our hands. An investigation of the relative energies of O–B π bonding versus P–B adduct formation is, thus, restricted to **2c**, which bears an OEt substituent at only one of its boron centers. This compound shows no sign of thermally-induced *ansa*-bridge opening up to 100 °C (NMR spectroscopy; toluene-*d*₈).

When **2a** is treated with Lipz, one bridging PPh₂ unit is displaced by the heterocyclic amine to give **3a**. Derivatives **2** with exocyclic pyrazole substituents are

apparently not existent. In contrast, the analogous reaction of **4a** with LiPPh₂ leads to the incorporation of PPh₂ groups into the *exo* positions of **4b** only. The pyrazole unit is fully maintained, and even after prolonged heating in boiling toluene, no rearrangement to the respective isomers **3** or **2** is observed. We, therefore, conclude that the pyrazole bridge is more stable than an interannular B₂P₂ ring. The reaction of **2a** with excess Lipz in THF/toluene (–78 °C to ambient temperature) stops at the stage of **3a**. Cleavage of the residual B–P bonds is apparently hampered by the presence of one pyrazole unit in the *ansa*-bridge.

Preliminary studies on the reactivity of compounds **2** toward transition metal Lewis acids reveal that the chromium center of Cr(CO)₅THF is not able to compete successfully with the boron atoms of **2a**, **2b**, and **2d** for the bridging phosphorus donors. No indication for *ansa*-bridge opening is found upon treatment of these compounds with the Cr(CO)₅ fragment, and in the case of **2d**, not even the exocyclic PPh₂ substituents act as ligands to the metal atom. However, with the assistance of a γ -picoline donor, *ansa*-**2a** is readily transformed into the heterotrimetallic Cr₂Fe complex **5b**. The potential of B–P-bridged ferrocenophanes as ligands to transition metals is the subject of further investigations in our laboratory.

Experimental Section

General Considerations. All reactions and manipulations of air-sensitive compounds were carried out in dry, oxygen-free argon using standard Schlenk ware or in an argon-filled drybox. Solvents were freshly distilled under N₂ from Na/K alloy–benzophenone (toluene, hexane, THF, Et₂O) or from CaH₂ (CH₂Cl₂, CH₃CN) prior to use. NMR: Jeol JMN-GX 400, Bruker DPX 400. ¹¹B NMR spectra are reported relative to external BF₃·Et₂O. ³¹P NMR shift values are given relative to external H₃PO₄ (85%). Unless stated otherwise, all NMR spectra were run at ambient temperature; abbreviations: s = singlet; d = doublet; tr = triplet; vtr = virtual triplet; q = quartet; br = broad; mult = multiplet; n.r. = multiplet expected in the ¹H NMR spectrum but not resolved; n.o. = signal not observed; Cp = cyclopentadienyl; bipy = 2,2'-bipyridine; pic = γ -picoline; pz = pyrazolyl; pz* = 4-bromo-3,5-dimethylpyrazolyl; the *ipso*, *ortho*, *meta*, and *para* positions of phenyl

(20) Forsén, S.; Hoffman, R. A. *J. Chem. Phys.* **1963**, *39*, 2892–2901.

(21) Forsén, S.; Hoffman, R. A. *Acta Chem. Scand.* **1963**, *17*, 1787–1788.

(22) Forsén, S.; Hoffman, R. A. *J. Chem. Phys.* **1964**, *40*, 1189–1196.

(23) Haaland, A. *Angew. Chem.* **1989**, *101*, 1017–1032; *Angew. Chem., Int. Ed. Engl.* **1989**, *28*, 992–1007.

rings are labeled as subscripts i, o, m, p (μ -PPh central), i', o', m', p' (μ -PPh close to ferrocene), and ie, oe, me, pe (exocyclic PPh₂); the cyclopentadienyl, pyrazolyl, and γ -picoline rings are numbered independently, following the numbering scheme of the parent heterocycle (see Schemes 3 and 4). Mass spectra (CI mode): Finnigan MAT 90. Elemental analyses: Micro-analytical laboratory of the *Technische Universität München*. The compounds **1a–e**,^{3,24} **2a,b**,⁴ and **4a**³ were synthesized according to literature procedures.

Synthesis of 2c. Method 1: **1d** (0.89 g, 1.95 mmol) in toluene (30 mL) was added dropwise with stirring to a suspension of LiPPh₂ (0.75 g, 3.90 mmol) in toluene (20 mL) at -78°C . After 30 min, the orange-red slurry was allowed to warm to ambient temperature, stirred for 12 h, and filtered through a frit (G4). The insoluble precipitate was extracted with toluene (2×10 mL). After all volatiles had been removed from the combined filtrates under reduced pressure, the orange-red oily residue was triturated with toluene/hexane (2:1; 25 mL) to afford **2c** as a yellow precipitate. **2c** was isolated by filtration and dried *in vacuo*. Yield: 0.55 g (35%).

Method 2: The ferrocene precursor **1c** was prepared *in situ* by adding diethyl ether (60 mg, 0.81 mmol) in toluene (10 mL) at ambient temperature to **1a** (0.42 g, 0.80 mmol) in toluene (20 mL). The solution was stirred for 7 days and evaporated to dryness under reduced pressure to remove bromoethane. The remaining **1c** was again dissolved in toluene (20 mL), cooled to -78°C , and added slowly with stirring to a slurry of LiPPh₂ (0.46 g, 2.39 mmol) in toluene (20 mL, -78°C). Further workup follows the procedure outlined above (method 1); the crude product was contaminated with **2d** (15%). Pure **2c** was obtained after recrystallization from toluene/hexane (2:1) at -25°C . Yield: 0.35 g (54%).

¹¹B NMR (128.3 MHz, CDCl₃): δ -8.4 ($h_{1/2} = 300$ Hz, BP-*exo*), 11.2 ($h_{1/2} = 400$ Hz, BO). ³¹P NMR (161.9 MHz, CDCl₃): δ -55.3 ($h_{1/2} = 150$ Hz, tr, 1P, ²J(P,P) = 35 Hz, P(*exo*)), -14.1 ($h_{1/2} = 200$ Hz, 2P, P(*u*)). ¹H NMR (400 MHz, CDCl₃): δ 1.39 (tr, 3H, ³J(H,H) = 6.7 Hz, OCH₂CH₃), 3.73 (n.r., 2H, Cp-H), 3.94 (q, 2H, ³J(H,H) = 6.7 Hz, OCH₂CH₃), 3.95 , 4.06 ($2 \times$ n.r., 4H, 2H, Cp-H), 6.91 (vtr, 4H, ³J(H,H) = 7.3 Hz, H_m), 6.99 (m, 10H, H_o, H_m, H_p), 7.17 (m, 2H, H_p), 7.32 (vtr, 4H, ³J(H,H) = 7.3 Hz, H_{me}), 7.38 (tr, 2H, ³J(H,H) = 7.3 Hz, H_{pe}), 8.00 (m, 4H, H_{oe}), 8.06 (br, 4H, H_o). ¹³C NMR (100.6 MHz, CDCl₃): δ 18.0 (OCH₂CH₃), 61.8 (br, OCH₂CH₃), 70.2 , 70.9 (Cp-C), 76.3 (tr, J(P,C) = 8 Hz, Cp-C), 77.0 (n.r., Cp-C), 127.0 (br, C_m, C_p), 127.9 (d, ³J(P,C) = 8 Hz, C_{me}), 128.4 (br, C_m, C_{pe}), 129.3 (br, C_p), 133.5 (br, C_o), 134.5 (d, ²J(P,C) = 17 Hz, C_o), 137.3 (d, ²J(P,C) = 22 Hz, C_{oe}), n.o. (Cp-C₁, Cp-C₁, C_i, C_i, C_{ie}). MS (CI): m/z 807 (7, MH⁺), 729 (10, M⁺ - Ph), 699 (20, MH⁺ - PPh). Anal. Calcd for C₄₈H₄₃B₂FeOP₃ (806.26): C, 71.51; H, 5.38; P, 11.53. Found: C, 71.38; H, 5.68; P, 11.13.

Synthesis of 2d. 1a (1.05 g, 2.00 mmol) in toluene (20 mL) was added dropwise with stirring to a slurry of LiPPh₂ (1.73 g, 9.00 mmol) in toluene (80 mL) at -78°C . After 30 min, the resulting reddish-brown mixture was allowed to warm to ambient temperature and stirred for 12 h. Insoluble LiBr was collected on a frit (G4) and extracted with toluene (2×10 mL). The combined filtrates were concentrated to a volume of 15 mL and kept at -25°C for several days, whereupon yellow microcrystalline **2d** gradually precipitated. After filtration, **2d** was washed with cold toluene (10 mL, -78°C) and dried *in vacuo* (24 h, 50°C). Yield: 1.64 g (87%). X-ray quality crystals of **2d**·1toluene were obtained from toluene/hexane (1:1) at -25°C .

¹¹B NMR (128.3 MHz, CDCl₃): δ -2.4 ($h_{1/2} = 500$ Hz). ³¹P NMR (161.9 MHz, CDCl₃): δ -57.9 (tr, ²J(P,P) = 31 Hz, P(*exo*)), -4.3 (n.r., $h_{1/2} = 100$ Hz, P(*u*)). ¹H NMR (400 MHz, CDCl₃): δ 3.73 , 4.10 ($2 \times$ n.r., $2 \times$ 4H, Cp-H), 6.13 (m, 4H, H_o), 6.70 (vtr, 4H, ³J(H,H) = 7.3 Hz, H_m), 7.07 (tr, 2H, ³J(H,H)

= 7.3 Hz, H_p), 7.17 (vtr, 4H, ³J(H,H) = 7.3 Hz, H_m), 7.25 (tr, 2H, ³J(H,H) = 7.3 Hz, H_p), 7.35 (vtr, 8H, ³J(H,H) = 7.3 Hz, H_{me}), 7.41 (tr, 4H, ³J(H,H) = 7.3 Hz, H_{pe}), 8.02 (br, 8H, H_{oe}), 8.38 (br, 4H, H_o). ¹³C NMR (100.6 MHz, CDCl₃): δ 70.2 (Cp-C), 77.8 (tr, J(P,C) = 8 Hz, Cp-C), 127.0 (vtr, ³J(P,C) = ⁵J(P,C) = 5 Hz, C_m), 127.9 (tr, ⁵J(P,C) = 5 Hz, C_{me}), 128.1 (vtr, ³J(P,C) = ⁵J(P,C) = 5 Hz, C_m), 128.5 (C_{pe}), 129.0 (C_p), 129.4 (C_p), 133.1 (vtr, ¹J(P,C) = ³J(P,C) = 19 Hz, C_i, C_i), 133.5 (vtr, ²J(P,C) = ⁴J(P,C) = 5 Hz, C_o), 135.3 (vtr, ¹J(P,C) = ³J(P,C) = 35 Hz, C_i, C_i), 135.6 (m, C_o), 137.4 (m, C_{oe}), 139.4 (m, C_{ie}), n.o. (Cp-C₁). Anal. Calcd for C₅₈H₄₈B₂FeP₄ (946.38): C, 73.61; H, 5.11, Fe 5.90, P 13.09. Found: C, 73.23; H, 5.31; Fe, 6.01; P, 12.85.

Synthesis of 2e. 1e (0.74 g, 1.46 mmol) in toluene (10 mL) was added slowly with stirring to a slurry of LiPPh₂ (0.59 g, 3.07 mmol) in toluene (30 mL) at -78°C . After 30 min, the orange mixture was allowed to warm to ambient temperature and stirred for 12 h. Insoluble LiBr was collected on a frit (G4) and extracted with toluene (2×10 mL). From the combined filtrates, the solvent was driven off under reduced pressure. Trituration of the orange oily residue with hexane (20 mL) afforded **2e** as a yellow solid. The crude product was isolated by filtration and recrystallized from toluene/hexane (1:10). Yield: 0.75 g (72%).

¹¹B NMR (128.3 MHz, CDCl₃): δ 42.9 ($h_{1/2} = 250$ Hz). ³¹P NMR (161.9 MHz, CDCl₃): δ -39.8 ($h_{1/2} = 50$ Hz). ¹H NMR (400 MHz, CDCl₃): δ 1.65 , 1.77 ($2 \times$ m, $2 \times$ 4H, NCH₂CH₂), 3.24 , 3.64 ($2 \times$ tr, $2 \times$ 4H, ³J(H,H) = 7.0 Hz, NCH₂CH₂), 3.94 , 4.05 ($2 \times$ vtr, $2 \times$ 4H, ³J(H,H) = ⁴J(H,H) = 1.7 Hz, Cp-H), 7.19 – 7.24 (m, 12H, H_m, H_p), 7.36 (m, 8H, H_o). ¹³C NMR (100.6 MHz, CDCl₃): δ 25.8 , 26.5 ($2 \times$ d, ⁴J(P,C) = 4 Hz, 6H, NCH₂CH₂), 50.9 , 51.5 ($2 \times$ d, ³J(P,C) = 4 Hz, 17 Hz, NCH₂CH₂), 71.8 (Cp-C), 75.8 (d, J(P,C) = 5 Hz, Cp-C), 127.0 (C_p), 128.2 (d, ³J(P,C) = 7 Hz, C_m), 134.5 (d, ²J(P,C) = 17 Hz, C_o), 138.1 (d, ¹J(P,C) = 8 Hz, C_i), n.o. (Cp-C₁). Anal. Calcd for C₄₂H₄₄B₂FeN₂P₂ (716.24): C, 70.43; H, 6.19; N, 3.91. Found: C, 70.11; H, 6.22; N, 3.78.

Synthesis of 3a. A cooled solution (-20°C) of **2a**·1toluene (0.25 g, 0.30 mmol) in toluene (25 mL) was added dropwise with stirring to a cold solution (-78°C) of Lipz (0.03 g, 0.41 mmol) in toluene/THF (1:1; 10 mL). The mixture was slowly warmed to ambient temperature, stirred for 12 h, and evaporated to dryness under reduced pressure. The yellow residue was washed with hexane (10 mL) and taken up in toluene (20 mL). Insoluble material was removed by filtration and the filtrate evaporated *in vacuo*. Recrystallization of the residue from toluene/hexane (1:1) afforded **3a**·1toluene (NMR spectroscopy; elemental analysis) as a yellow microcrystalline solid. Yield: 0.19 g (77%). The same product was obtained upon reaction of **2a**·1toluene with 2.5 equiv of Lipz.

¹¹B NMR (128.3 MHz, CDCl₃): δ -2.1 ($h_{1/2} = 500$ Hz). ³¹P NMR (161.9 MHz, CDCl₃): δ -46.6 (d, ²J(P,P) = 50 Hz, P(*exo*)), 0.9 ($h_{1/2} = 300$ Hz, P(*u*)). ¹H NMR (400 MHz, CDCl₃): δ 3.11 (m, 1H, Cp-H₂), 3.41 (m, 1H, Cp-H₂), 3.44 (m, 1H, Cp-H₅), 3.79 (m, 1H, Cp-H₅), 3.92 (m, 1H, Cp-H₄), 4.00 (m, 1H, Cp-H₃), 4.03 (m, 1H, Cp-H₃), 4.09 (m, 1H, Cp-H₄), 6.39 (m, 2H, H_o), 6.61 (m, 1H, pz-H₄), 7.07 (vtr, 4H, ³J(H,H) = 7.3 Hz, H_{me}), 7.10 – 7.30 (m, 6H, H_{pe}, H_m, H_o), 7.31 (tr, 1H, ³J(H,H) = 7.3 Hz, H_p), 7.37 (m, 2H, H_m), 7.44 (m, 4H, H_{oe}), 7.58 (tr, 1H, ³J(H,H) = 7.3 Hz, H_p), 7.63 , 8.33 ($2 \times$ d, $2 \times$ 1H, ³J(H,H) = 1.8 Hz, pz-H₃, pz-H₅). ¹³C NMR (100.6 MHz, CDCl₃): δ 69.2 (d, ⁴J(P,C) = 1 Hz, Cp-C₃), 70.5 (d, ⁴J(P,C) = 1 Hz, Cp-C₃), 71.1 (Cp-C₄), 71.3 (Cp-C₄), 71.4 (d, ³J(P,C) = 8 Hz, Cp-C₂), 73.0 (d, ³J(P,C) = 9 Hz, Cp-C₂), 73.3 (Cp-C₅), 75.0 (Cp-C₅), 108.2 (d, ⁴J(P,C) = 4 Hz, pz-C₄), 127.5 – 128.0 (m, C_{pe}, C_{me}), 128.3 , 128.8 ($2 \times$ d, ³J(P,C) = 11 Hz, C_m, C_m), 130.1 (d, ⁴J(P,C) = 1 Hz, C_p), 132.1 (d, ⁴J(P,C) = 1 Hz, C_p), 132.6 (d, ²J(P,C) = 6 Hz, C_o), 135.3 (d, ²J(P,C) = 20 Hz, C_o), 136.0 (d, ³J(P,C) = 8 Hz, pz-C₃, pz-C₅), 136.3 (d, ²J(P,C) = 20 Hz, C_{oe}), 136.7 (br, pz-C₃, pz-C₅), n.o. (Cp-C₁, Cp-C₁, C_i, C_i, C_{ie}). Anal. Calcd for C₃₇H₃₁B₂BrFeN₂P₂·1.0 C₇H₈ (815.13): C, 64.83; H, 4.82; N, 3.44. Found: C, 65.13; H, 5.03; N, 3.72.

Synthesis of 3b and 3c. **2a**·1toluene (0.39 g, 0.47 mmol) in toluene (30 mL) was added dropwise with stirring at ambient temperature to a slurry of Lipz* (0.10 g, 0.55 mmol) in diethyl ether (20 mL). The resulting yellow solution was stirred for 12 h and evaporated to dryness. The yellow oil obtained was treated with hexane (10 mL), whereupon it solidified. The precipitate was extracted with toluene (20 mL), and the volatiles were removed from the filtrate under reduced pressure. Recrystallization of the solid residue from toluene/hexane (1:1) at $-20\text{ }^{\circ}\text{C}$ gave yellow X-ray quality crystals of **3c**·0.5toluene·0.25 hexane. Yield: 0.10 g (27%). The mother liquor was layered with half its volume of hexane and kept at $-20\text{ }^{\circ}\text{C}$ to afford **3b**·1toluene as a microcrystalline yellow solid. Yield: 0.21 g (48%).

3b: ^{11}B NMR (128.3 MHz, CDCl_3): δ -2.3 ($h_{1/2}$ = 400 Hz). ^{31}P NMR (161.9 MHz, CDCl_3): δ -43.7 (d, $^2J(\text{P},\text{P})$ = 40 Hz, $\text{P}(\text{exo})$), -6.3 ($h_{1/2}$ = 300 Hz, $\text{P}(\mu)$). ^1H NMR (400 MHz, CDCl_3): δ 2.18, 2.83 (2 \times s, 2 \times 3H, CH_3), 3.02 (m, 1H, Cp-H₂), 3.37 (m, 1H, Cp-H₂), 3.46 (m, 1H, Cp-H₅), 3.81 (m, 1H, Cp-H₅), 3.92 (m, 1H, Cp-H₄), 4.02, 4.04 (2 \times m, 2 \times 1H, Cp-H₃, Cp-H₃), 4.12 (m, 1H, Cp-H₄), 6.99 (vtr, 4H, $^3J(\text{H},\text{H})$ = 7.3 Hz, H_{me}), 7.08 (m, 2H, H_{pe}), 7.15–7.35 (m, 9H, H_0 , H_m , H_p , H_o , H_n), 7.44 (m, 4H, H_{oe}), 7.61 (tr, 1H, $^3J(\text{H},\text{H})$ = 7.3 Hz, H_p). ^{13}C NMR (100.6 MHz, CDCl_3): δ 13.7 (d, $^4J(\text{P},\text{C})$ = 10 Hz, CH_3) 14.6 (CH_3), 69.7 (d, $^4J(\text{P},\text{C})$ = 2 Hz, Cp-C₃), 70.5 (Cp-C₃), 71.4 (d, $^3J(\text{P},\text{C})$ = 7 Hz, Cp-C₂, Cp-C₂), 71.5, 71.5 (Cp-C₄, Cp-C₄), 71.7 (d, $^3J(\text{P},\text{C})$ = 9 Hz, Cp-C₂, Cp-C₂), 73.3, 74.0 (Cp-C₅, Cp-C₅), 99.8 (d, $^4J(\text{P},\text{C})$ = 6 Hz, pz-C₄), 127.8 (d, $^3J(\text{P},\text{C})$ = 7 Hz, C_{me}), 128.2 (d, $^3J(\text{P},\text{C})$ = 10 Hz, C_{m} , C_{m}), 128.5 (C_{pe}), 128.7 (d, $^3J(\text{P},\text{C})$ = 10 Hz, C_{m} , C_{m}), 130.3 (d, $^4J(\text{P},\text{C})$ = 3 Hz, C_p), 132.1 (d, $^4J(\text{P},\text{C})$ = 3 Hz, C_p), 133.1 (d, $^2J(\text{P},\text{C})$ = 6 Hz, C_0), 134.0 (d, $^2J(\text{P},\text{C})$ = 16 Hz, C_0), 136.1 (m, C_{oe}), 146.7 (d, $^3J(\text{P},\text{C})$ = 8 Hz, pz-C₃, pz-C₅), 147.1 (d, $^3J(\text{P},\text{C})$ = 7 Hz, pz-C₃, pz-C₅), n.o. (Cp-C₁, Cp-C₁, C_i, C_r, C_{ie}). Anal. Calcd for $\text{C}_{39}\text{H}_{34}\text{B}_2\text{Br}_2\text{FeN}_2\text{P}_2\cdot\text{C}_7\text{H}_8$ (922.08): C, 59.92; H, 4.59; N, 3.04. Found: C, 60.21; H, 4.50; N, 3.22.

3c: ^{11}B NMR (128.3 MHz, CDCl_3) δ -3.0 ($h_{1/2}$ = 400 Hz). ^{31}P NMR (161.9 MHz, CDCl_3): δ -10.0 ($h_{1/2}$ = 350 Hz). ^1H NMR (400 MHz, CDCl_3): δ 2.76 (s, 6H, CH_3), 3.36 (n.r., 2H, Cp-H₂, Cp-H₂), 3.82 (n.r., 2H, Cp-H₅, Cp-H₅), 4.01 (n.r., 2H, Cp-H₄, Cp-H₄), 4.07 (n.r., 2H, Cp-H₃, Cp-H₃), 6.73 (m, 2H, H_0), 7.27 (vtr, 2H, $^3J(\text{H},\text{H})$ = 7.4 Hz, H_{m}), 7.36 (tr, 1H, $^3J(\text{H},\text{H})$ = 7.4 Hz, H_p), 7.69 (vtr, 2H, $^3J(\text{H},\text{H})$ = 7.4 Hz, H_{m}), 7.77 (tr, 1H, $^3J(\text{H},\text{H})$ = 7.4 Hz, H_p), 8.40 (m, 2H, H_o). ^{13}C NMR (100.6 MHz, CDCl_3): δ 13.9 (CH_3), 70.4 (Cp-C₃, Cp-C₃), 71.3 (d, $^3J(\text{P},\text{C})$ = 8 Hz, Cp-C₂, Cp-C₂), 72.0 (Cp-C₄, Cp-C₄), 73.4 (Cp-C₅, Cp-C₅), 100.3 (d, $^4J(\text{P},\text{C})$ = 7 Hz, pz-C₄), 128.5 (d, $^3J(\text{P},\text{C})$ = 10 Hz, C_{m}), 129.3 (d, $^3J(\text{P},\text{C})$ = 11 Hz, C_{m}), 130.3 (d, $^4J(\text{P},\text{C})$ = 3 Hz, C_p), 132.4 (d, $^2J(\text{P},\text{C})$ = 7 Hz, C_0), 133.1 (d, $^4J(\text{P},\text{C})$ = 2 Hz, C_p), 135.6 (d, $^2J(\text{P},\text{C})$ = 7 Hz, C_0), 147.1 (d, $^3J(\text{P},\text{C})$ = 8 Hz, pz-C₃, pz-C₅), n.o. (Cp-C₁, Cp-C₁, C_i, C_r). MS (CI): m/z 722 (100, M⁺), 537 (74, M⁺ - PPh₂). Anal. Calcd for $\text{C}_{27}\text{H}_{24}\text{B}_2\text{Br}_2\text{FeN}_2\text{P}_2\cdot 0.5\text{C}_7\text{H}_8\cdot 0.25\text{C}_6\text{H}_{14}$ (792.28): C, 48.51; H, 3.98; N, 3.54. Found: C, 48.34; H, 3.99; N, 3.61.

Synthesis of 4b. **4a** (0.31 g, 0.62 mmol) in toluene (40 mL) was added at ambient temperature with stirring to a slurry of LiPPh₂ (0.26 g, 1.35 mmol) in toluene (10 mL). The mixture was refluxed for 12 h to afford a yellow solution and a white precipitate, which was removed by filtration. The filtrate was evaporated under reduced pressure, and the yellow solid residue was washed with hexane (10 mL). Recrystallization of the crude product from toluene/hexane (1:7) gave yellow crystals of **4b**. Yield: 0.36 g (82 %).

^{11}B NMR (128.3 MHz, CDCl_3): δ 0.7 ($h_{1/2}$ = 300 Hz). ^{31}P NMR (161.9 MHz, CDCl_3): δ -39.3 ($h_{1/2}$ = 40 Hz). ^1H NMR (400 MHz, C_6D_6): δ 3.21 (vtr, 4H, $^3J(\text{H},\text{H})$ = $^4J(\text{H},\text{H})$ = 1.7 Hz, Cp-H₂, Cp-H₅), 4.04 (vtr, 4H, $^3J(\text{H},\text{H})$ = $^4J(\text{H},\text{H})$ = 1.7 Hz, Cp-H₃, Cp-H₄), 5.51 (tr, 2H, $^3J(\text{H},\text{H})$ = 1.8 Hz, pz-H₄), 7.00 (tr, 4H, $^3J(\text{H},\text{H})$ = 7.3 Hz, H_p), 7.08 (m, 8H, H_{m}), 7.39 (m, 8H, H_0), 8.07 (d, 4H, $^3J(\text{H},\text{H})$ = 1.8 Hz, pz-H₃, pz-H₅). ^{13}C NMR (100.6 MHz, C_6D_6): δ 70.5 (Cp-C₃, Cp-C₄), 72.0 (Cp-C₂, Cp-C₅), 106.2 (pz-C₄), 127.0 (C_p), 128.4 (d, $^3J(\text{P},\text{C})$ = 6

Hz, C_{m}), 133.7 (d, $^2J(\text{P},\text{C})$ = 15 Hz, C_0), 137.2 (d, $^1J(\text{P},\text{C})$ = 14 Hz, C_i), 137.6 (d, $^3J(\text{P},\text{C})$ = 15 Hz, pz-C₃, pz-C₅), n.o. (Cp-C₁, Cp-C₁). MS (CI): m/z 526 (100, M⁺ - PPh₂). Anal. Calcd for $\text{C}_{40}\text{H}_{34}\text{B}_2\text{FeN}_4\text{P}_2$ (710.15): C, 67.65; H, 4.83; N, 7.89; P, 8.72. Found: C, 68.06; H, 4.88; N, 7.62; P, 8.38.

Synthesis of 5a. γ -Picoline (5 mL) was added to **2a**·1toluene (1.66 g, 2.00 mmol) at ambient temperature with stirring. A clear red solution was obtained within 30 min, from which a yellow microcrystalline solid gradually precipitated over a period of several hours. The slurry was diluted with toluene (20 mL), and all of the insoluble material was collected on a frit, treated subsequently with toluene (2 \times 20 mL) and hexane (2 \times 20 mL), and dried *in vacuo*. **5a**·1toluene was obtained in a yield of 2.09 g (87%).

^{11}B NMR (128.3 MHz, CDCl_3): δ 7.3 ($h_{1/2}$ = 500 Hz). ^{31}P NMR (161.9 MHz, CDCl_3): δ -27.4 ($h_{1/2}$ = 50 Hz). ^1H NMR (400 MHz, CDCl_3): δ 2.67 (s, 12H, CH_3), 3.23, 4.20 (2 \times n.r., 2 \times 4H, Cp-H), 6.90 (vtr, 8H, $^3J(\text{H},\text{H})$ = $^3J(\text{H},\text{P})$ = 7.3 Hz, H_0), 7.16 (vtr, 8H, $^3J(\text{H},\text{H})$ = 7.3 Hz, H_{m}), 7.28 (tr, 4H, $^3J(\text{H},\text{H})$ = 7.3 Hz, H_p), 7.72 (d, 8H, $^3J(\text{H},\text{H})$ = 5.8 Hz, pic-H_{3,5}), 8.52 (d, 8H, $^3J(\text{H},\text{H})$ = 5.8 Hz, pic-H_{2,6}). ^{13}C NMR (100.6 MHz, CDCl_3): δ 21.7 (CH_3), 72.0 (d, $^3J(\text{P},\text{C})$ = 2.3 Hz, Cp-C_{2,5}), 73.3 (Cp-C_{3,4}), 80.8 (br, Cp-C₁), 127.5 (pic-C_{3,5}), 127.8 (C_p), 128.1 (d, $^3J(\text{P},\text{C})$ = 7.7 Hz, C_{m}), 133.5 (d, $^2J(\text{P},\text{C})$ = 17.7 Hz, C_0), 135.1 (d, $^1J(\text{P},\text{C})$ = 13.1 Hz, C_i), 144.8 (d, $^3J(\text{P},\text{C})$ = 7.7 Hz, pic-C_{2,6}), 157.5 (pic-C₄). Anal. Calcd for $\text{C}_{58}\text{H}_{56}\text{B}_2\text{Br}_2\text{FeN}_4\text{P}_2\cdot\text{C}_7\text{H}_8$ (1200.48): C, 65.03; H, 5.37; N, 4.67; Br, 13.31. Found: C, 64.74; H, 5.40; N, 4.93; Br, 13.09.

Synthesis of 5b. **5a**·1toluene (0.24 g, 0.20 mmol) was dissolved in toluene/ CH_2Cl_2 (1:1; 20 mL), and 28 mL (1.29 mmol) of a freshly prepared and calibrated solution of $\text{Cr}(\text{CO})_5$ (THF) in THF was added at ambient temperature. The mixture was stirred for 24 h, and the solvents were removed under reduced pressure. Trituration of the yellow crude product with toluene (2 \times 10 mL) and hexane (2 \times 10 mL) afforded **5b** as a yellow microcrystalline solid. Yield: 0.24 g (80%).

^{11}B NMR (128.3 MHz, CD_2Cl_2): δ 8.4 ($h_{1/2}$ = 500 Hz). ^{31}P NMR (161.9 MHz, CD_2Cl_2): δ 19.3 ($h_{1/2}$ = 80 Hz). ^1H NMR (400 MHz, CD_2Cl_2): δ 2.73 (s, 12H, CH_3), 3.52, 3.78 (2 \times br, 2 \times 4H, Cp-H), 7.13 (br, 8H, H_0), 7.25 (vtr, 8H, $^3J(\text{H},\text{H})$ = 7.3 Hz, H_{m}), 7.41 (tr, 4H, $^3J(\text{H},\text{H})$ = 7.3 Hz, H_p), 7.78 (br, 8H, pic-H_{3,5}), 8.53 (br, 8H, pic-H_{2,6}). ^{13}C NMR (100.6 MHz, CD_2Cl_2): δ 26.0 (CH_3), 68.1, 73.0 (Cp-C), 128.7 (pic-C_{3,5}), 129.0 (d, $^3J(\text{P},\text{C})$ = 7.8 Hz, C_{m}), 130.3 (C_p), 134.6 (d, $^2J(\text{P},\text{C})$ = 8.7 Hz, C_0), 146.2 (pic-C_{2,6}), 160.5 (pic-C₄), 217.0 (d, $^2J(\text{P},\text{C})$ = 7.8 Hz, CO_{eq}), 225.5 (CO_{ax}), n.o. (Cp-C₁, C_i). M_w for $\text{C}_{68}\text{H}_{56}\text{B}_2\text{Br}_2\text{Cr}_2\text{FeN}_4\text{O}_{10}\text{P}_2$: 1492.44.

Crystal Structure Determination of 2d(toluene).¹⁷ A yellow crystal of **2d**·toluene was selected in a perfluorinated oil and mounted in a glass capillary on an image plate diffraction system (IPDS, STOE). Final lattice parameters were obtained by least-squares refinement of 1935 reflections (graphite monochromator, λ = 0.710 73 Å, MoK α). Empirical formula $\text{C}_{58}\text{H}_{48}\text{B}_2\text{FeP}_4\cdot\text{C}_7\text{H}_8$, fw = 1038.45, monoclinic system, space group $C2/c$ (No. 15); a = 36.522(3) Å, b = 13.566(1) Å, c = 22.181(2) Å, β = 96.133(7)°, V = 10926.8(16) Å³, crystal size 0.45 \times 0.33 \times 0.25 mm, D_{calc} = 1.262 g cm⁻³, Z = 8, $F(000)$ = 4336. Data were collected at 253 \pm 2 K, distance from crystal to image plate 75 mm ($2.3^\circ < \theta < 24.7^\circ$), 270 images collected, $0^\circ < \varphi < 270^\circ$, $\Delta\varphi$ = 1°, exposure time 2.5 min. Data were corrected for Lorentz and polarization effects.²⁵ A decay and absorption correction (μ = 4.3 cm⁻¹) was performed using the program DECAY;²⁵ 61 576 data were measured, and 9100 independent reflections were used for refinement. The structure was solved by direct methods and refined with standard difference Fourier techniques. All hydrogen atoms of **2d** were calculated in ideal positions (riding model); hydrogen atoms of the disordered toluene molecules were not considered.

(25) IPDS Operating System Version 2.6.; STOE&CIE; GmbH: Darmstadt, Germany, 1995.

Number of parameters refined: 685, 13.3 data per parameter, weighting scheme $w = 1/[\sigma^2(F_o^2) + (0.0703P)^2 + 10.5115P]$, where $P = (F_o^2 + 2F_c^2)/3$, shift/error < 0.001 in the last cycle of refinement, residual electron density +0.92 e Å⁻³, -0.22 e Å⁻³, R1 = 0.0566 (all data), wR2 = 0.1191 (all data), minimized function was $\Sigma w(F_o^2 - F_c^2)^2$. Neutral atom scattering factors for all atoms and anomalous dispersion corrections for the non-hydrogen atoms were taken from the International Tables for X-Ray Crystallography.²⁶ All calculations were performed on a DEC 3000 AXP workstation with the STRUX-V system,²⁷ including the programs PLATON-92,²⁸ PLUTON-92,²⁸ SHELXS-86,²⁹ SIR-92,³⁰ and SHELXL-93.³¹

Crystal Structure Determination of 3c·0.5(toluene)·0.25(hexane).¹⁷ A yellow crystal of 3c·0.5toluene·0.25 hexane was selected in a perfluorinated oil and mounted in a glass capillary on an image plate diffraction system (IPDS, STOE). Final lattice parameters were obtained by least-squares refinement of 1975 reflections (graphite monochromator, $\lambda = 0.71073$ Å, MoK α). Empirical formula C₂₇H₂₄B₂Br₃FeN₂P·0.5 C₇H₈·0.25C₆H₁₄, fw = 770.72 + 0.25C₆H₁₄, tetragonal system, space group *P*4₂/*m* (No. 84); *a* = 15.8389(9) Å, *b* = 15.8389(9) Å, *c* = 12.6240(6) Å, *V* = 3167.0(3) Å³, crystal size 0.43 × 0.25 × 0.13 mm, *D*_{calcd} = 1.617 g cm⁻³, *Z* = 4, *F*(000) = 1524. Data were collected at 193 ± 2 K, distance from crystal to image plate 70 mm (2.1° < θ < 25.6°), 120 images collected, 0° < φ < 120°, $\Delta\varphi = 1^\circ$, exposure time 1 min. Data were corrected for Lorentz and polarization terms.²⁵ A decay and absorption

correction ($\mu = 43.3$ cm⁻¹) was performed using the program DECAY.²⁵ 14 259 data were measured, and 2984 independent reflections were used for refinement. The structure was solved by direct methods and refined with standard difference Fourier techniques. All hydrogen atoms of 3c and toluene were calculated in ideal positions (riding model). The gross structure and location of the disordered hexane molecules were confirmed. Further refinement to any satisfactory level was not possible. We have, therefore, applied the “squeeze” routine³² (ca. 15 e⁻ suppressed) to cure this disordered solvent problem. Number of parameters refined: 200, 14.9 data per parameter, weighting scheme $w = 1/[\sigma^2(F_o^2) + (0.0873P)^2]$, where $P = (F_o^2 + 2F_c^2)/3$, shift/error < 0.001 in the last cycle of refinement, residual electron density +1.57 e Å⁻³, -1.33 e Å⁻³, R1 = 0.0811 (all data), wR2 = 0.1483 (all data), minimized function was $\Sigma w(F_o^2 - F_c^2)^2$. Neutral atom scattering factors for all atoms and anomalous dispersion corrections for the non-hydrogen atoms were taken from the International Tables for X-Ray Crystallography.²⁶ All calculations were performed on a DEC 3000 AXP workstation with the STRUX-V system,²⁷ including the programs PLATON-92,²⁸ PLUTON-92,²⁸ SHELXS-86,²⁹ SIR-92,³⁰ and SHELXL-93.³¹

Acknowledgment. We are grateful to Prof. Dr. W. A. Herrmann (Technische Universität München) for his generous support and to the “Deutsche Forschungsgemeinschaft” and the “Fonds der Chemischen Industrie” for financial funding.

Supporting Information Available: Tables of X-ray parameters, atomic coordinates and thermal parameters, and bond distances and angles for 2d and 3c (18 pages). Ordering information is given on any current masthead page.

OM970484G

(32) Spek, A. SQUEEZE. An effective cure for the disordered solvent syndrome in crystal structure refinement. *ACA-94*; Atlanta, GA, 1994; Abstract M05, p 66.

(26) *International Tables for Crystallography*; Wilson, A. J. C., Ed.; Kluwer Academic Publishers: Dordrecht, The Netherlands, 1992; Vol. C, Tables 4.2.4.2, 4.2.6.8, 6.1.1.4, pp 193–199, 219–222, 500–502.

(27) Artus, G.; Scherer, W.; Priermeier, T.; Herdtweck, E. *STRUX-V, A Program System to Handle X-ray Data*; TU München: München, Germany, 1994.

(28) Spek, A. L. *Acta Crystallogr.* **1990**, *A46*, C34.

(29) Sheldrick, G. M. *SHELXS-86: Program for Crystal Structure Solutions*; Universität Göttingen: Göttingen, Germany, 1986.

(30) Altomare, A.; Cascarano, G.; Giacovazzo, C.; Guagliardi, A.; Burla, M. C.; Polidori, G.; Camalli, M. *SIR-92*; University of Bari: Italy.

(31) Sheldrick, G. M. *J. Appl. Crystallogr.*, *in press*.